Far infrared spectroscopy of the B335 region

B.Nisini[1], T.Giannini[1], C.Ceccarelli[1,2], R.Liseau[3], D. Lorenzetti[4], S.Molinari[1,5], P.Saraceno[1], L.Spinoglio[1], S.J.Leeks[6], D.Naylor[7], G.J. White[6]

[1] *CNR-Istituto di Fisica dello Spazio Interplanetario - CP 27, I-00044 - Frascati, Italy*

[2] *Laboratoire d'Astrophysique, Observatoire de Grenoble - BP 53, F-38041 Grenoble cedex, France*

[3] *Stockholm Observatory - S-133 36, Saltsjöbaden, Sweden*

[4] *Osservatorio Astronomico di Roma - I-00040 Monteporzio, Italy*

[5] *LIDT, ISO Science Operations Centre - P.O. Box 50727, 28080 Madrid, Spain*

[6] *Physics Department, Queen Mary & Westfield College, Mile End Road - London E1 4NS, UK*

[7] *Department of Physics, University of Lethbridge - Lethbridge, Alberta T1K 3M4, Canada*

bruni@taurus.ifsi.fra.cnr.it

Abstract

We present far infrared spectra, obtained with the Long Wavelength Spectrometer (LWS) onboard the ISO satellite, on the B335 dark cloud region. In particular, deep integration spectra were acquired on the far infrared outflow exciting source, located in the B335 core, and on the three associated Herbig Haro (HH) objects HH119 A, B and C. In addition, we mapped a region of about 12′ in RA and 5′ in DEC covering the whole molecular outflow.

A [CII]157μm emission uniformely distributed in all the region is observed, with the intensity expected for a photodissociation region excited by the average interstellar field. The [OI]63μm emission is detected only from the HH objects and from the B335 FIR source; the observed line intensity is in agreement with the existing shock models. CO line emission from the rotational level J=15 to J=18 are detected in B335 FIR only: we model this emission as due to a compact (7x10^{-3} pc), warm (T=150 K) and dense (n$_{H_2}$ = 4x10^6 cm^{-3}) region. We think that such a warm gas cannot be excited in the collapsing envelope as modelled for this source. Finally, we find that the thermal emission of the FIR source could be fitted by a model assuming a free-fall density distribution law $\rho \propto r^{-1.5}$, although a flatter density profile ($r^{-0.5}$) produces a much better fit with the LWS spectrum shortward of 60μm.

1. Introduction

The dark globule B335, located at a distance of 250pc, appears in the POSS prints as an opaque region extended 2′ EW and 3′ NS (Frerking et al. 1987). It contains a well collimated bipolar outflow oriented almost perpendicular to the line of sight with an estimated dynamical age of about 2x10^4 yr (Moriarty-Schieven et al. 1989, Hirano et al. 1992).

The outflow exciting source was identified in a low-luminosity (L = 2.9 L$_\odot$) far-infrared/sub-millimeter object (B335 FIR), associated with the IRAS source IRAS19345+0727 (Chandler et al. 1990), in the center of a dense core of about 30″ of diameter (Frerking et al. 1987). From the analysis of the profiles of CS and H$_2$CO lines, Zhou et al.(1993) suggested that this core is still collapsing.

The small scale structure of the protostellar core was studied through high resolution observations of ^{12}CO, other CO isotopics and millimeter continuum observations (Hirano et al. 1992, Chandler & Sargent 1993). They resolved a condensation of about 10″ with density of 3×10^6 cm^{-3}, and a total mass of about 0.2M$_\odot$, *i.e.* $\sim$ 5% of the total mass of the B335 core.

Three HH objects, HH119A, B and C, have been found in the outflow, aligned , together with the FIR source, along the outflow axis (Reipurth et al. 1992). HH119 B and C are at the same distance from the FIR source, in opposite directions, while HH119A is further away from the source in the outflow red-lobe.

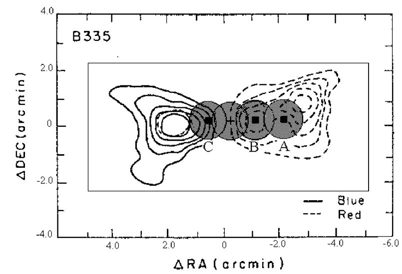

Fig. 1.— The ISO-LWS pointing positions are superimposed on the CO outflow map in B335. The cross and the squares indicate the position of the far-infrared source and of the three HH119 objects (A, B and C) respectively. The rectangular area outlines the region of the raster map.

2. Observations and results

We observed the B335 region with ISO-LWS (Clegg et al. 1996) in grating mode (43-196.7um at a resolution of $\sim$ 200 and with a beamsize of about 80″), during revolutions 181 and 316.

We obtained grating specta of B335 FIR (19^h 34^m 35.3^s +07^o 27′ 24″), and of the three HH objects 119A, B and C, integrating 40 sec for each spectral element: in addition, we made a raster map of 7x3 LWS beams spaced 100″ each other, centered on the FIR source (see Fig.1), integrating 6.4 sec per spectral element. All the spectra were oversampled by a factor 4 and they were calibrated using observations of Uranus with an estimated accuracy better than 30% (Swinyard et al. 1996).

Toward B335 FIR we detected emission from [OI]63μm and 145μm, [CII]157μm and from the four CO rotational transitions with upper J= 15, 16, 17 and 18. On the three HH objects we detected only [OI]63μm and [CII]157μm (Fig.2 and 3).

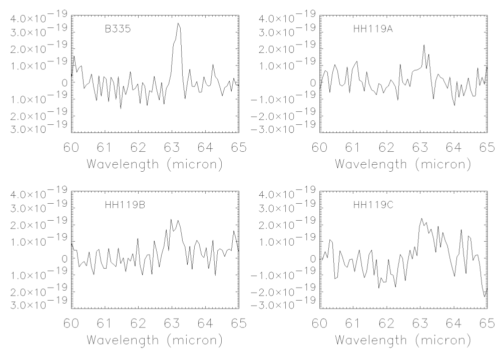

Fig. 2.— Continuum subtracted [OI]63μm line spectra in B335 and the three HH objects.

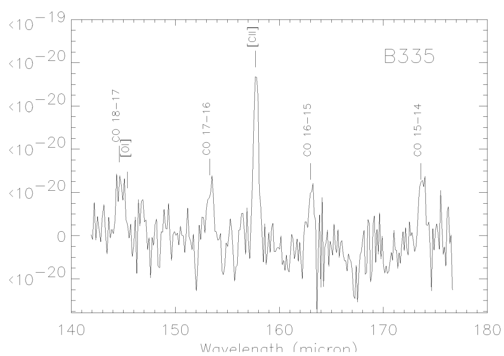

Fig. 3.— Continuum subtracted LW4 spectrum of B335 which shows the detected CO and [CII]157μm lines.

3. Discussion

3.1. The [CII]157μm emission

The raster map spectra show that the [CII]157μm line emission has a comparable flux in all the positions with an average value of $[4.8\pm0.4]\times10^{-20}$ W cm^{-2}, as expected by a diffuse PDR region excited by the interstellar UV field (see also Nisini et al. 1996). Moreover the observed line intensity is consistent with a medium with density $\sim 3\times10^3$ cm^{-3} (like measured in B335, Frerking et al. 1987) illuminated by a FUV field of about 1G$_0$ (Hollenbach et al. 1991). This picture is also consistent with the 2σ upper limit of 2.1×10^{-20} W cm^{-2} we obtain for the [OI]63μm diffuse emission averaging all the spectra of the raster map. We do not observe any increase of [CII] on the FIR source, implying that no PDR excess emission arises from the central object.

3.2. The [OI]63μm emission

The three HH objects have a comparable [OI]63μm line emission (average value $[7.2\pm0.1]\times10^{-20}$ W cm^{-2}) while on B335 FIR we measure a slightly larger flux ($[1.2\pm0.2]\times10^{-19}$ W cm^{-2}). We also averaged together seven map spectra along the outflow axis, obtaining an outflow spectrum at an integration time larger than in the HHs and B335 FIR pointings; we do not detect any 63μm emission here which indicates that almost all the [OI] emission is confined in the region covered by our pointed observations. Since this localized emission does not come from the diffuse PDR responsible for the [CII] emission, it has to be almost entirely due to shock excitation.

We assume that the [OI] has been excited by the same shock interactions which have originated the HHs knots. Such knots are travelling at $\sim$ 200 km s^{-1} (Reipurth et al.1992), in a medium which have a density of about 3×10^3 cm^{-3} (Frerking et al. 1987). According to Hollenbach and McKee (1989), a shock with such velocity and pre-shock density should produce a 63μm intensity of $\sim 10^{-13}$ $n_o \cdot v_s = 6\times10^{-10}$Wcm^{-2} sr^{-1}. In order to compare this number with the observed flux it has to be multiplied by the dimension of the emitting region. Such a region cannot be smaller than the size of the optical HH knots that can be estimated (Reipurth et al. (1992)) to be of about $\sim 3''$ of diameter, *i.e.* 1.6×10^{-10} sr. We therefore have an estimated [OI]63μm line emission of about 9×10^{-20}Wcm^{-2} not very different from the observed value. Our observations are therefore consistent with a fast shock excitation in a very compact region around the HH objects. The larger flux observed on B335 FIR could be justified by a larger pre-shock density as observed in the inner part of the molecular core.

3.3. The CO emission

To interpret the emission of the high-J CO lines observed by ISO-LWS we have used an LVG code, with a plane-parallel geometry, in which the collisional excitation rates from McKee et al. (1982) were assumed. An intrinsic line width of 8 km s^{-1} has been used, consistent with the observed width of the CO J=6$\rightarrow$5 transition (Ceccarelli et al.1997). The best fit found is given by a model with a gas temperature of 150 K, a density of 4×10^6 cm^{-3} and a hydrogen column density (assuming X(CO)/X(H$_2$) = 1×10^{-4}) equal to 8×10^{22} cm^{-2} (Fig.5). The derived column density implies a filling factor of the order of 7×10^{-2}, which indicates that the emission is coming from a compact region of about 5.5$''$ of diameter. The total mass of this warm gas component is about 1.5×10^{-2} M$_\odot$. The fact that we seem to observe the peak of this CO emission component make the derived fit rather stringent. A much colder gas cannot be excited at such high rotational levels, while the upper limits derived on the J=19 and J=20 lines imply that this gas cannot be much warmer or more diffuse than what we find in our fit. To compare our fit results with other observations, we report in Fig. 4 the emission from the CO J=6$\rightarrow$5 line observed at JCMT by Ceccarelli et al. (1997): the authors made a cross scan through B335 FIR finding that the emission from this line is extended in a region of about 20$''$ of diameter. We can see that the total observed flux from this line is well above our fit: in fact, it resulted impossible to fit both the 6$\rightarrow$5 and the high-J line emission with a single gas component. We can compare our results

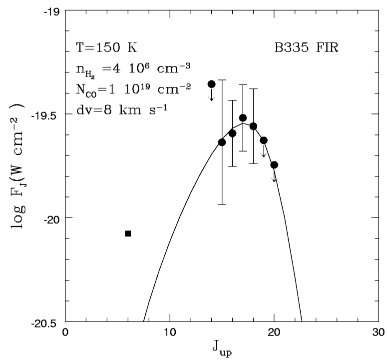

Fig. 4.— Model fit of the observed CO line fluxes. Filled circles refer to LWS observations while the filled square indicates the CO 6→5 observed at JCMT. Upper limits are at 2σ.

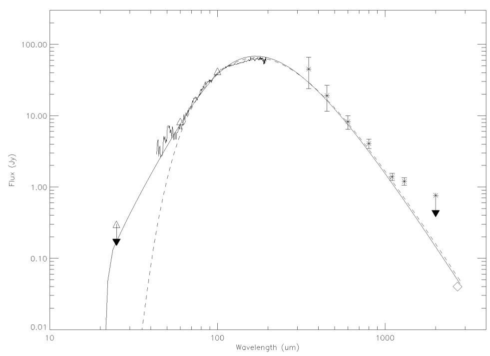

Fig. 5.— Model fit of the continuum spectrum of B335. The ISO-LWS spectrum is plotted together with submillimiter data taken from Chandler et al. (1990) (stars), the 2.7mm observation by Chandler and Sargent (1993) (diamond) and the IRAS fluxes (triangles). The dashed line is the best fit model obtained assuming a free-fall density distribution law, while the solid line represents a fit with a density distribution law $\propto r^{-0.5}$.

with the collapsing core model for B335 by Zhou et al. (1993). The density found by our fit in a 5.5″ region is consistent with the average density implied by their best-fit density distribution which assume a 1.5 power law (i.e. 2×10^6 cm^{-3}). The Zhou et al. model, however, assumes that the gas temperature remains very low (about 10-15 K) even at very inner radii inside the envelope (less than 0.005pc corresponding to 4″) which is in contradiction with the presence of the warm CO we are probing here. Given the low radiation field expected from the protostellar source, excitation by a low velocity, non-dissociative shock is the more likely mechanism from which this warm gas emission component can be originated.

3.4. The continuum emission

The thermal emission spectrum of B335 is shown in Fig. 5 where the ISO-LWS data spectrum is plotted together with ground-based observations and IRAS fluxes. The observed energy distribution of B335 is fitted with a model of a spherically symmetric dust envelope in which density and temperature T vary according to radial power laws $\rho \propto r^{-q}$ and T $\propto r^{-p}$ respectively. Boundary conditions on T and ρ are set at the outer envelope radius (T_{out}, ρ_{out}). A dust mass opacity of 0.1 cm^2 g^{-1} at 250μm (Hildebrand 1983) is assumed with a frequency dependence represented by a power law with exponent β. Following Chandler et al. (1990), we take an outer envelope radius of 50″ corresponding to 0.03pc. Since the dust continuum emission of B335 has been succesfully modelled by a density distribution law typical of infalling envelopes (Chandler and Sargent 1993, Zhou et al. 1990) we have fixed the parameter q equal to 1.5 finding a best-fit model, shown in Fig.5 as dashed line, with the following parameters: ρ_{out} = 6.0 10^{-21} g cm^{-3}, T_{out}=13 K, p = 0.24 and β=1.75. These parameters imply a total gas+dust envelope mass (assuming a gas-to-dust ratio of 100) of 1.85 $M_\odot$. This model, which is in agreement with that found by Zhou et al., falls very steeply shortward of 60μm failing to match the LWS spectrum in this region. To fit also the short wavelength part of the spectrum with a spherical model a density power law shallower than the 1.5 value is needed: in Fig. 5 is shown as solid line the model obtained leaving the density power law free to vary: in this case we obtain q = 0.5, p = 0.3, ρ_{out} = 9.0 10^{-21} g cm^{-3} while the other parameters and the total mass remain unchanged.

REFERENCES

Ceccarelli C., Boogert A., Tielens A.G.G.M. 1997, in preparation

Candler C.J. et al. 1990, MNRAS 243, 330

Chandler C.J., Sargent A.I. 1993, ApJ 414, L29

Clegg P.E. et al. 1996, A&A 315, L38

Frerking M.A., Langer W.D., Wilson R.W. 1987, ApJ 313, 320

Hildebrand R.H. 1983, QJRAS 24, 267

Hirano N., Kameya O., Kasuga T., Umemoto Y. 1992, ApJ 390, L85

Hollenbach D., Takahashi T., Tielens A.G.G.M. 1991, ApJ 377, 192

Hollenbach D. & McKee C.F. 1989, ApJ 342,306

McKee C.F., Storey J.W.V., Watson D.M., Green S. 1982, ApJ 259, 647

Moriarty-Schieven G.H. & Snell R.L. 1989, ApJ 338, 952

Nisini et al. 1996, A&A 315, L321

Reipurth B., Heathcote S., Vrba F. 1992, A&A 256, 225

Swinyard et al. 1996, A&A 315, L43

Zhou S., Evans N.J., Kömpe C., Walmsley C.M. 1993, ApJ 404, 232